The American Journal of Pathology, Vol. 180, No. 4, April 2012

DOI: 10.1016/j.ajpath.2011.12.041

Neurobiology

Ferroxidase Hephaestin's Cell-Autonomous Role in the Retinal Pigment Epithelium

Natalie Wolkow, Delu Song, Ying Song, Sally Chu, Majda Hadziahmetovic, Jennifer C. Lee, Jared Iacovelli, Steven Grieco, and Joshua L. Dunaief

From the F.M. Kirby Center for Molecular Ophthalmology, Scheie Eye Institute, Perelman School of Medicine at the University of Pennsylvania, Philadelphia, Pennsylvania

Hephaestin (Heph) is a ferroxidase protein that converts ferrous to ferric iron to facilitate cellular iron export by ferroportin. Many tissues express either Heph or its homologue, ceruloplasmin (Cp), but the retina expresses both. In mice, a combined systemic mutation of Heph and systemic knockout of Cp ($Cp^{-/-}$, $Heph^{sla/sla}$) causes retinal iron accumulation and retinal degeneration, with features of human age-related macular degeneration; however, the role of Heph and Cp in the individual retinal cells is unclear. Herein, we used conditional knockout mice to study Heph's role in retinal pigment epithelial (RPE) and photoreceptor cells. Loss of both Heph and Cp from RPE cells alone results in RPE cell iron accumulation and degeneration. We found, however, that RPE iron accumulation in these conditional knockout mice is not as great as in systemic knockout mice. Photoreceptor-specific Heph knockout indicates that the additional iron in the RPE cells does not result from loss of ferroxidases in the photoreceptors, and Cp and Heph play minor roles in photoreceptors. Instead, loss of ferroxidases in other retinal cells causes retinal iron accumulation and transfer of iron to the RPE cells. Cp and Heph are necessary for iron export from the retina but are not essential for iron import into the retina. Thus, our studies, revise how we think about iron import and export from the retina. ***(Am J Pathol 2012, 180:1614–1624; DOI: 10.1016/j.ajpath.2011.12.041)***

Hephaestin (Heph) and ceruloplasmin (Cp) are homologous ferroxidase proteins[1] that convert ferrous to ferric iron to facilitate cellular iron export by ferroportin.[2,3] Many tissues express either Heph or Cp, but the retina expresses both,[4] suggesting that maintenance of appropriate iron levels is important to the retina. Several proteins that are critical for normal vision, such as RPE65, contain iron as a cofactor.[5] Furthermore, iron overload can cause retinal disease, as seen in the autosomal recessive disease, aceruloplasminemia,[6] and in age-related macular degeneration,[7] in which iron levels are elevated, especially in the retinal pigment epithelial (RPE) cells.

The retina is composed of neural cells (photoreceptors, bipolar, horizontal, amacrine, and ganglion cells), which detect and propagate light signal, and support cells (RPE, astrocytes, and Muller cells) (Figure 1A). The RPE cells are critical for vision because they recycle components of the visual cascade and phagocytose portions of photoreceptor outer segments on a daily basis.[8,9] Dysfunction of RPE cells can result in photoreceptor degeneration and blindness.[10,11]

Previous studies[4] have shown that Heph is present in RPE and Muller cells. In addition, recent immunofluorescence studies have suggested that Heph is expressed in photoreceptors (unpublished data). Cp is present in the RPE cells and in both glycophosphatidylinositol-linked and secreted forms in the neural retina[4,12]; in light-damaged retinas, Cp is up-regulated in Muller cells.[12] Systemic knockout of *Cp* ($Cp^{-/-}$) or systemic mutation of *Heph* ($Heph^{sla/sla}$) alone results in minimal or no retinal iron accumulation.[4,13] However, when both *Cp* is systemically knocked out and *Heph* is systemically mutated ($Cp^{-/-}$, $Heph^{sla/sla}$), iron accumulates in the retina and a retinal degeneration with features of human age-related macular degeneration develops,[4] suggesting that, in the retina, Cp and Heph are essential and have overlapping functions.

Supported by a grant from the NIH (F30 AG037289 to N.W.; RO1 EY015240 to J.L.D.), an unrestricted grant from Research to Prevent Blindness (J.L.D.), the F.M. Kirby Foundation (J.L.D.), a gift in memory of Lee F. Mauger, M.D. (J.L.D.), and the Paul and Evanina Bell Mackall Foundation Trust (J.L.D.).

Accepted for publication December 20, 2011.

Address reprint requests to Joshua L. Dunaief, M.D., Ph.D., F.M. Kirby Center for Molecular Ophthalmology, Scheie Eye Institute, Perelman School of Medicine at the University of Pennsylvania, 305 Stellar-Chance Laboratory, 422 Curie Blvd, Philadelphia, PA 19104. E-mail: jdunaief@mail.med.upenn.edu.

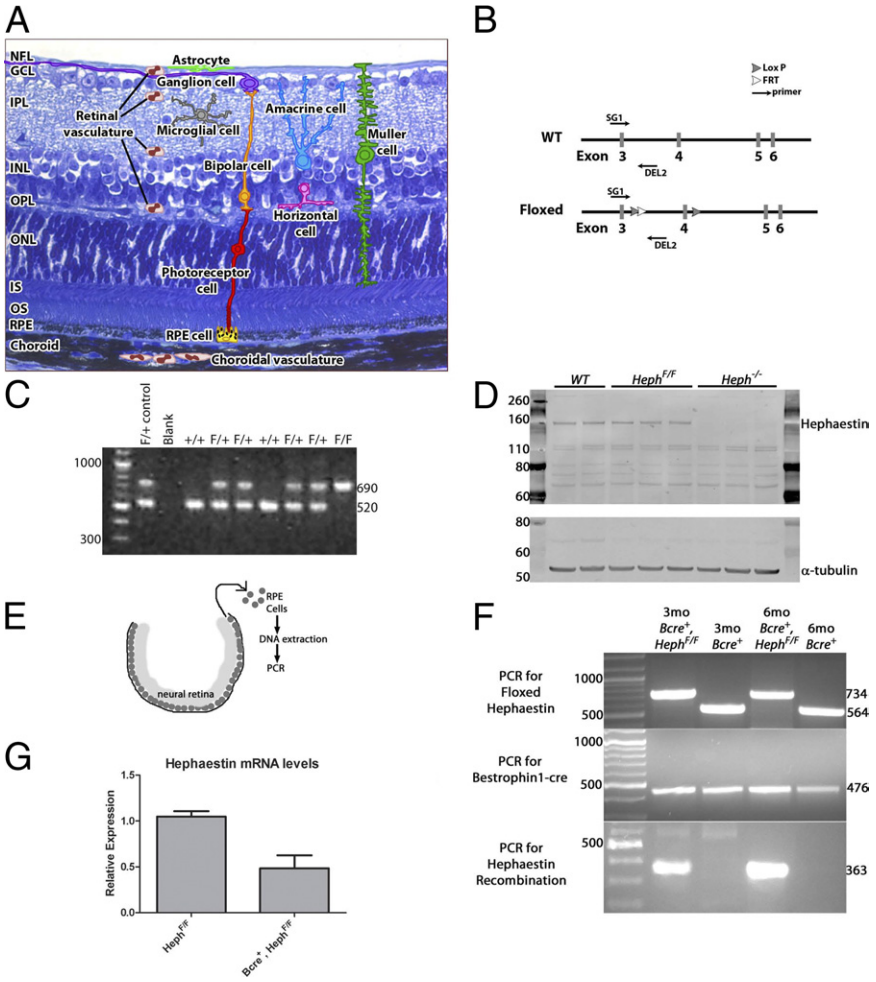

Figure 1. A: Structure of the retina. RPE, photoreceptor, bipolar, ganglion, Muller, amacrine, horizontal, and microglial cells and astrocytes are indicated, as are the retinal and choroidal blood vessels. GCL, ganglion cell layer; INL, inner nuclear layer; IPL, inner plexiform layer; IS, inner segments; NFL, nerve fiber layer; ONL, outer nuclear layer; OPL, outer plexiform layer; OS, outer segments. **B:** Schematic of the WT *Heph* gene and the floxed *Heph* gene. LoxP and FRT insertion sites are indicated. Primers used for floxed *Heph* genotyping are indicated. **C:** PCR showing WT (564 bp) and floxed (734 bp) *Heph* products. Primers SG1 and Del2 were used. **D:** Western blot analysis for Heph (161 kDa) on neural retinas from 7-month-old WT, $Heph^{F/F}$, and $Heph^{-/-}$ mice. Loading control, α-tubulin (55 kDa). **E:** Schematic illustrating RPE cell isolation. **F:** PCR for floxed *Heph*, *Bestrophin1-cre*, and *Heph* recombination on DNA extracted from isolated RPE cells. **G:** Quantitative RT-PCR for Heph exon 4 mRNA on RNA from isolated RPE cells. A Satterthwaite two-sample *t*-test was used to compare the means. $P = 0.003$.

The $Cp^{-/-}$, $Heph^{sla/sla}$ mice have increased iron levels throughout the entire neural retina, but as in aceruloplasminemia, the largest iron accumulation is in the RPE cells.[4,6] This suggests that Cp and Heph function is especially critical in the RPE cells. Although it is apparent from the $Cp^{-/-}$, $Heph^{sla/sla}$ mice that Cp and Heph are important for retinal iron homeostasis, their roles in the individual retinal cell types and in the directionality of retinal iron transport are unclear. To address these questions, we developed *Heph* conditional knockout mice to determine Heph's role in the RPE and other retinal cells.

Materials and Methods

Mice

Floxed *hephaestin* ($Heph^{F/F}$) mice were generated with the inGenious Targeting Laboratory, Inc. (Stony Brook, NY). *Exon 4*, which contains critical copper-binding domains that are important for Heph's function, was floxed; its deletion also results in a frameshift. The *Heph* gene sequence was identified in the RPCI-23 (C57Bl/6J; Minako Tateno) mouse BAC library (Kazutoyo Osoegawa and M. Tateno, Children's Hospital Oakland Research Institute, Oakland, CA) and subcloned into a pSP72 (Promega, Madison, WI) vector. A single *loxP* site was inserted downstream of *exon 4*, and a *loxP/FRP*-flanked *Neo* cassette was inserted upstream of *exon 4*. The targeting vector was electroporated into iTL IC1 (*C57Bl/6*; inGenious Targeting Laboratory, Inc., Ronkonkoma, NY) embryonic stem cells. Targeted stem cells with homologous recombination were microinjected into *BALB/c* blastocysts. Chimeric progeny were mated to *wild-type* (*WT*) *C57Bl/6* mice to generate F_1 heterozygous offspring. The presence of the transgene and *loxP* sites were confirmed with Southern blotting and PCR in the F_1 offspring, and confirmed mice were mated with *C57Bl/6 FLP* mice to remove the *Neo* cassette. F_2 mice were screened for the deletion of the *Neo* cassette and retention of the distal *loxP* site by PCR. Mice that had *Neo* deletion and the *loxP* present were further mated to *WT C57Bl/6* mice. F_3 mice were screened for *Neo* deletion and absence of the *FLP* transgene. Once mice were generated with *Neo* deletion and absence of *FLP*, they were bred to each other to generate homozygous $Heph^{F/F}$ mice. PCR for floxed *hephaestin* was performed using the following primers: Del2, 5′-GAATCATGTACACATCCACTTTACAGA-3′; and SG1, 5′-TCAGCAATGAAGCACCTTAGC-3′. The annealing temperature was

55°C. The expected band size for the *WT* allele was 520 bp; and for the floxed allele, 690 bp.

Heph$^{F/F}$ mice were mated to *Bestrophin1-cre* or *Rhodopsin1-cre* mice to delete *Heph exon 4* specifically from the RPE or photoreceptor cells or the retina, respectively. *Bestrophin1-cre* (*Bcre*$^{+}$) mice, which express cre specifically in the RPE cells, have been previously described.[14] *Rhodopsin-cre* (*Rcre*$^{+}$) mice, which express cre specifically in the photoreceptor cells of the retina, have been previously described.[15] *Bcre*$^{+}$, *Heph*$^{F/F}$ and *Rcre*$^{+}$, *Heph*$^{F/F}$ mice were also bred with systemic *ceruloplasmin* knockout (*Cp*$^{-/-}$) mice, which have been previously described,[16] to generate *Bcre*$^{+}$, *Cp*$^{-/-}$, *Heph*$^{F/F}$ and *Rcre*$^{+}$, *Cp*$^{-/-}$, *Heph*$^{F/F}$ mice.

In addition, *Heph*$^{-/-}$ mice were generated by taking advantage of occasional ectopic cre expression in the testes of *Bcre*$^{+}$, *Heph*$^{F/F}$ mice. *Bcre*$^{+}$, *Heph*$^{F/F}$ mice were bred to one another, and some progeny had evidence of systemic *Heph* recombination by PCR. These progeny were mated to one another and then bred to remove the *Bcre*$^{+}$ transgene. The *Heph*$^{-/-}$ mice were bred to *Cp*$^{-/-}$ mice to generate *Cp*$^{-/-}$, *Heph*$^{-/-}$ mice. *Cp*$^{-/-}$, *Heph*$^{sla/sla}$ mice were also used and have been previously described.[4] All mice were handled in accordance with the Institutional Animal Care and Use Committee of the University of Pennsylvania, Philadelphia. For all experiments, mice were sacrificed with CO_2 inhalation, followed by cervical dislocation.

RPE Cell Isolation

RPE cells were isolated from other ocular structures using enzymatic (dispase and hyaluronidase) digestion and mechanical dissection, as previously described.[17]

DNA Extraction and PCR

DNA was extracted from RPE cells using the QIAGEN QIAamp DNA Micro kit (catalogue number 56304; Qiagen, Valencia, CA) and from other tissues using the QIAGEN DNeasy Blood and Tissue kit (catalogue number 69504; Qiagen), as recommended by the manufacturer. PCR for floxed *hephaestin* was performed using the following primers: forward, 5′-CTTTGGACCACACATGCAAC-3′; and reverse, 5′-AAAACCCAGCTCCTCCATTT-3′. The annealing temperature was 51°C. The expected band size for the *WT* allele was 564 bp; and for the floxed allele, 734 bp. PCR for *hephaestin* recombination was performed using the following primers: forward, 5′-GACAAGAGCTCTAGGAGAGATGCCA-3′; and reverse, 5′-CCAAGCATTCAGTAGACCTAGGAAGGA-3′. The annealing temperature was 58.5°C. The expected band size for recombination was 363 bp. PCRs for *Bestrophin1-cre* and *Rhodopsin-cre* were performed in one reaction using the following primers: Rcre forward, 5′-TGGGGACTGGATAAGTCAGG-3′; Vcre forward, 5′-CCGTTGCTTCTGAGCAGATT-3′; and Cre reverse, 5′-CGGTTATTCAACTTGCACCA-3′. The annealing temperature was 56°C. The expected band sizes were 476 bp for Bestrophin1-Cre and 600 bp for Rhodopsin-Cre. A PCR for *Cp* was performed using the following primers: ACp-16, 5′-CATACTCTGAACACCCTGAGAAAG-3′; ACp-17, 5′-CATCAGATACCAGTTGACTTCATC-3′; and ACp-neo2, 5′-GCTCTTTACTGAAGGCTCTTTACT-3′. The annealing temperature was 65°C. The expected band size was 500 bp for the *WT* allele and 800 bp for the knockout allele. For the *Heph* recombination PCR, Fermentas DreamTaq PCR reagents were used (Fermentas, Glen Burnie, MD); for all other PCRs, AmpliTaqGold DNA Polymerase and appropriate buffers (Applied Biosystems, Carlsbad, CA) were used.

RNA Extraction and Quantitative RT-PCR

RNA was extracted from isolated RPE cells using the QIAGEN RNeasy Plus Micro kit (catalogue number 74034; Qiagen) and QIAshredder columns (catalogue 79654; Qiagen) and from primary Muller cells using the QIAGEN RNeasy Mini Kit (catalogue number 74106) and QIAshredder columns, as recommended by the manufacturer. cDNA was synthesized using Taqman Reverse Transcription reagents (catalogue N808-0234; Applied Biosystems, Carlsbad). Quantitative PCR was performed on a 7500 Fast Real-Time PCR System Thermocycler (Applied Biosystems, Foster City, CA), using the following Taqman probes: ferroportin (Slc40a1, Mm00489837_m1), hephaestin (Mm00515970_m1), ceruloplasmin (Mm00432654_m1), transferrin receptor (Mm00441941_m1), zyklopen (Zp; Hephl1, Mm03990837_m1∗), amyloid precursor protein (APP; Mm01344172_m1∗), RPE65 (Mm00504133_m1), hepcidin (Mm00519025_m1), hemopexin (Mm00457510_m1∗), transferrin (Mm00446708_m1∗), and custom probe HEPHEX4. The sequences for primers were as follows: forward, 5′-AGGAATACAGTGATGGCACATACAC-3′; reverse, 5′-GCCTGTAACAGTGGTCCTAGGAA-3′; and probe, 5′-AGGCTTGGCTATTTC-3′) (Applied Biosystems, Carlsbad), as suggested by the manufacturer.

Immunofluorescence

Mouse eyes were enucleated; fixed in 4% paraformaldehyde for 2 hours; dissected to remove the cornea, iris, and lens; cryoprotected overnight in 30% sucrose; and cryoembedded in Tissue-Tek Optimal Cutting Temperature Compound (Sakura Finetek, Torrance, CA). Cryosections (10 μm thick) were immunostained, as previously described.[18] Primary antibodies used were rabbit anti-L-ferritin and rabbit anti-H-ferritin at 1:2500 dilutions (gifts from Paolo Arosio, Universita degli Studi di Brescia, Brescia, Italy), mouse anti-cre recombinase at a 1:500 dilution (MAB3120; Millipore, Billerica, MA), mouse anti-protein kinase Cα at a 1:500 dilution (BD-Pharmingen, Franklin Lakes, NJ), and mouse anti-glutamine synthetase at a 1:250 dilution (ab64613; Abcam, Cambridge, MA). Slides were examined on a Nikon Eclipse 80i microscope (Nikon Instruments, Melville, NY), and images were acquired using NIS-BR Elements version 4.1 software (Nikon Instruments).

Histological Analysis

Mouse eyes were enucleated, fixed in 2% paraformaldehyde–2% glutaraldehyde overnight, and embedded in JB-4 plastic (Polysciences, Warrington, PA) plastic. Sec-

tions (3 μm thick) were stained with toluidine blue, as previously described.[18]

Perls' Stain

Perls' stain for iron was performed on plastic sections (3 μm thick), as previously described.[4,18] Both unenhanced and VECTOR VIP Peroxidase Substrate Kit - enhanced (SK-4600, Vector Laboratories, Burlingame, CA) Perls' staining was performed.

Primary Muller Cell Culture

Primary Muller cells were cultured, as previously described.[17] Muller cell identity was verified using quantitative RT-PCR for RPE65 and immunofluorescence for cellular retinaldehyde binding protein and vimentin, as previously described.[17]

Western Blot Analysis

Eyes from 7-month-old mice of different genotypes were dissected by separating neurosensory retina from the underlying RPE/choroid and sclera. Dissected retinas were frozen on dry ice and stored at −80°C. For Western blot analysis after homogenization, the retinas were lysed in radioimmunoprecipitation assay buffer and protein was quantified using the BCA Protein Assay Kit (Thermo Scientific, Rockford, IL). Total protein (20 μg) was used in each lane. The samples were incubated in loading buffer for 10 minutes at 70°C. Protein lysates were separated on a 4% to 12% SDS-PAGE gel and transferred to a nitrocellulose membrane. Blocking was achieved by incubation in Tris-buffered saline containing 5% milk and 0.1% Tween 20. Membranes were incubated overnight at 4°C with rabbit anti-mouse Heph IgG antibody at 1:2000 dilution (catalogue number HEPH11-A; α Diagnostics, San Antonio, TX). After washes, membranes were incubated with anti-rabbit IgG at 1:5000 dilution (GE Healthcare, Piscataway, NJ) and developed using ECL Plus reagent (GE Healthcare, Piscataway, NJ). Anti-α-tubulin antibody (Sigma-Aldrich, Inc., St Louis, MO) was used as a loading control. Images were acquired using a Typhoon 9400 Variable Mode Imager (GE Healthcare), and densitometry was performed using ImageQuant TL (GE Healthcare).

Statistical Analysis

Experiments were performed in triplicate. The mean ± SE values were calculated for each comparison group. The means were compared using either a Satterthwaite two-sample *t*-test or a one-way analysis of variance, followed by a Tukey post test. $P < 0.05$ was considered to be statistically significant. Data are reported as the mean ± SEM. All statistical analysis was performed with GraphPad Prism software version 5 (GraphPad Software, San Diego, CA).

Results

Generation of Heph$^{F/F}$ *and* Bcre^{+}, Heph$^{F/F}$ *Mice*

Mice with floxed *Heph exon 4* (Heph$^{F/F}$) were generated (Figure 1, B and C). Disruption of this exon results in the loss of a critical copper-binding site and a frameshift near the 5′ end of the coding sequence, causing the loss of Heph protein. In retinas of mice with systemic cre-mediated recombination (*Heph*$^{-/-}$), Heph protein was undetectable (Figure 1D).

To determine hephaestin's role in the RPE cells, *Heph*$^{F/F}$ mice were bred to *Bestrophin1-cre* (*Bcre*$^{+}$) mice[14] that target cre specifically to the RPE cells of the retina. On the *C57Bl/6* background, cre is expressed in 50% to 90% of RPE cells.[14] Cre expression in the RPE cells of *Bcre*$^{+}$, *Heph*$^{F/F}$ mice resulted in *hephaestin* DNA recombination (Figure 1, E and F) and Heph mRNA decrease (Figure 1G) in RPE cells alone. Complete Heph mRNA elimination was not expected because of the mosaic expression of cre in RPE cells.

Bcre^{+}, Heph$^{F/F}$ *Mice Do Not Have Increased RPE Iron Levels*

Cp$^{-/-}$, *Heph*$^{sla/sla}$ mice have increased RPE iron accumulation, despite low circulating iron levels (M. Hadziahmetovic, J.L. Dunaief, unpublished data). Because *Bcre*$^{+}$, *Heph*$^{F/F}$ mice have normal circulating iron levels, we hypothesized that loss of Heph alone from the RPE may result in RPE iron accumulation. However, there was no increase in RPE iron levels in *Bcre*$^{+}$, *Heph*$^{F/F}$ mice up to the age of 18 months, as determined by Perls' stain for iron and immunofluorescence for the iron storage proteins, L- and H-ferritin (data not shown), demonstrating that alternative iron export mechanisms can compensate for Heph's loss in the RPE.

Bcre^{+}, Cp$^{-/-}$, Heph$^{F/F}$ *Mice Accumulate RPE Iron*

To determine whether Cp was compensating for Heph's absence in RPE cells, *Bcre*$^{+}$, *Heph*$^{F/F}$ mice were bred onto a systemic *Cp*$^{-/-}$ background to generate *Bcre*$^{+}$, *Cp*$^{-/-}$, *Heph*$^{F/F}$ mice. *Cp*$^{-/-}$ mice were used, rather than floxed *Cp*, because Cp is present in both membrane-bound and secreted forms in the retina.[12] *Bcre*$^{+}$, Cp$^{-/-}$, *Heph*$^{F/F}$ mice had increased iron levels in cre-positive RPE cells, as determined by immunofluorescence for L-ferritin (Figure 2, A and B); this change was first seen at the age of 3 months and was only present in cre-positive cells. No changes in ferritin immunostaining were detected in the neural retina (data not shown). Transferrin receptor levels were decreased in both isolated RPE cells and neural retinas of *Bcre*$^{+}$, *Cp*$^{-/-}$, *Heph*$^{F/F}$ mice, indicating that labile iron levels were increased in these tissues and demonstrating that the neural retina does not depend on iron import from the choroid and RPE (Figure 2C).

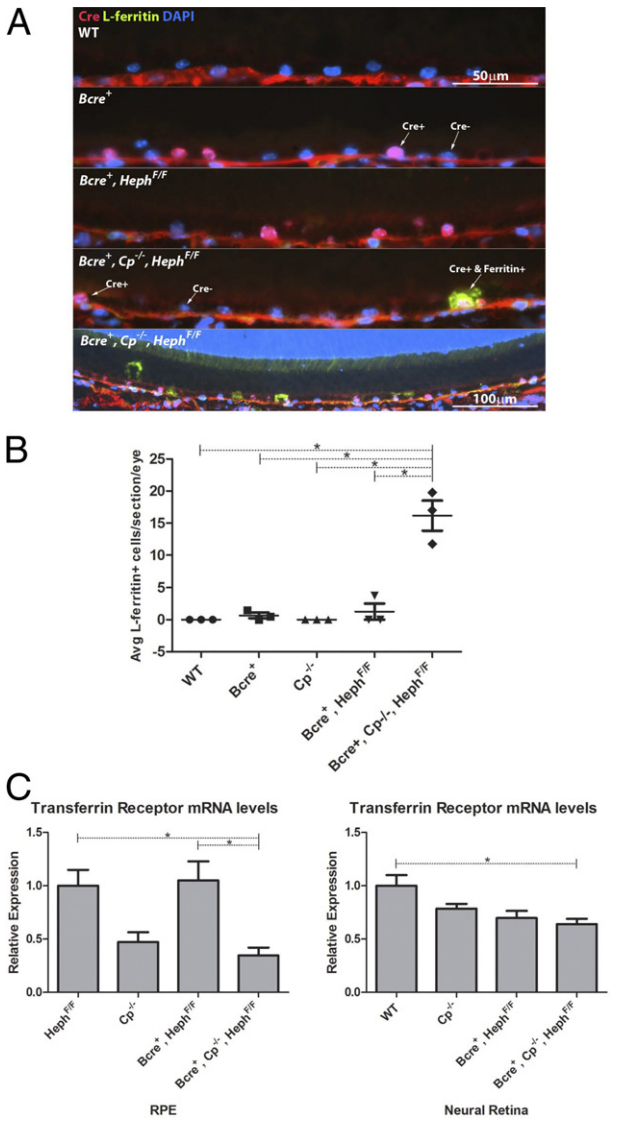

Figure 2. A: Representative images of immunofluorescence for cre (red) and L-ferritin (green) on RPE cells of 9-month-old mice of different genotypes. Only cre-positive cells of *Bcre*$^{+}$, *Cp*$^{-/-}$, *Heph*$^{F/F}$ mice have increased L-ferritin levels. **B:** Quantification of L-ferritin–positive cells. Four slides from three mice of each genotype were assessed. The average number of L-ferritin–positive cells per slide for each mouse is plotted on the graph. A one-way analysis of variance with a Tukey post test was used to compare the means between the groups. $P < 0.0001$ for all indicated comparisons. **C:** Quantitative RT-PCR for transferrin receptor on RNA from isolated RPE cells and RNA extracted from neural retinas. A one-way analysis of variance with a Tukey post test was used to compare the means between the groups. $P = 0.0052$ for indicated comparisons in the RPE graph, and $P = 0.0093$ for indicated comparisons in the neural retina graph. The **asterisk** denotes that a significant difference exists between the means of the indicated groups.

Iron Accumulation in Bcre^{+}, Cp$^{-/-}$, Heph$^{F/F}$ *RPE Cells Causes Pathological Changes*

In addition to increased RPE iron levels, *Bcre*$^{+}$, *Cp*$^{-/-}$, *Heph*$^{F/F}$ mice had areas of RPE cell atrophy, RPE hypertrophy, large vacuoles, and RPE cells that had extruded into the photoreceptor layer (Figure 3, A–D, respectively). The extruded RPE cells were always cre positive (Figure 3E). Thus, moderately increased iron levels in RPE cells are sufficient to cause RPE pathological characteristics.

Bcre^{+}, *Cp*$^{-/-}$, *Heph*$^{F/F}$ RPE cells do not accumulate as much iron as *Cp*$^{-/-}$, *Heph*$^{sla/sla}$ RPE cells; RPE cells in *Cp*$^{-/-}$, *Heph*$^{sla/sla}$ mice still have residual Heph ferroxidase function, but cre-positive RPE cells in *Bcre*$^{+}$, *Cp*$^{-/-}$, *Heph*$^{F/F}$ mice should not. Thus, the *Bcre*$^{+}$, *Cp*$^{-/-}$, *Heph*$^{F/F}$ cre-positive RPE cells should have more iron accumulation than *Cp*$^{-/-}$, *Heph*$^{sla/sla}$ RPE cells if RPE cell iron accumulation is only dependent on the cell-autonomous roles of Cp and Heph. However, RPE cells in *Bcre*$^{+}$, *Cp*$^{-/-}$, *Heph*$^{F/F}$ mice had less iron than *Cp*$^{-/-}$, *Heph*$^{sla/sla}$ mice at all ages, as determined by immunofluorescence for L- and H-ferritin and by Perls' stain for iron (Figure 4, A and B). In addition, unlike *Cp*$^{-/-}$, *Heph*$^{sla/sla}$ mice, the *Bcre*$^{+}$, *Cp*$^{-/-}$, *Heph*$^{F/F}$ RPE cells were not autofluorescent (Figure 4C), indicating that moderately increased RPE iron levels are not sufficient to cause autofluorescence, even though they cause other RPE pathological characteristics. Furthermore, these results suggested that the high iron levels in the RPE cells of *Cp*$^{-/-}$, *Heph*$^{sla/sla}$ mice must come from other retinal cells that lack Heph function.

Heph Plays Only a Minor Role in Photoreceptors

Because RPE cells phagocytose photoreceptor outer segments on a daily basis, and photoreceptors have increased iron levels in *Cp*$^{-/-}$, *Heph*$^{sla/sla}$ mice, phagocytosis of iron-laden photoreceptors is a potential mechanism for iron transfer to RPE cells in *Cp*$^{-/-}$, *Heph*$^{sla/sla}$ mice. In addition, loss of Cp and Heph from photoreceptor cells may result in photoreceptor iron accumulation. To determine Heph's role in photoreceptor cells, *Heph*$^{F/F}$ mice were bred to *Rcre*$^{+}$ mice, which target cre to the photoreceptors. *Rcre*$^{+}$, *Heph*$^{F/F}$ mice had no photoreceptor iron accumulation up to 18 months (data not shown). Similarly, *Rcre*$^{+}$, *Cp*$^{-/-}$, *Heph*$^{F/F}$ mice had no changes in retinal iron levels compared with controls and had no retinal pathological characteristics (data not shown).

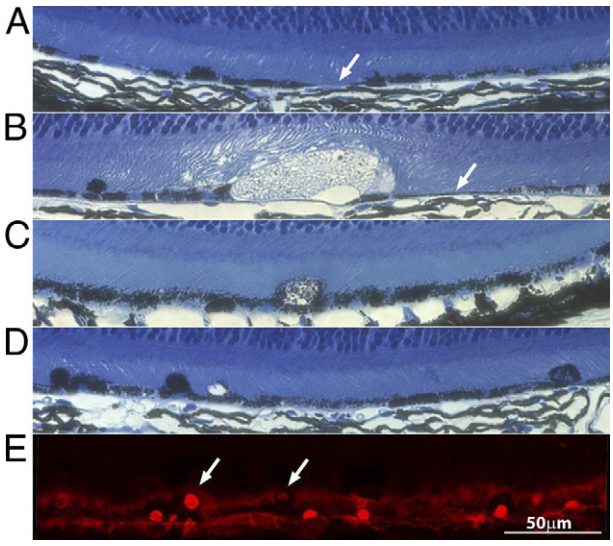

Figure 3. A: Area of RPE cell atrophy (**arrow**). **B:** A large vacuole, extruded RPE cell, and area of RPE atrophy (**arrow**). **C:** A hypertrophic RPE cell. **D:** Extruded RPE cells in a 6-month-old *Bcre*$^{+}$, *Cp*$^{-/-}$, *Heph*$^{F/F}$ mouse. **E:** Extruded RPE cells (**arrows**) are cre positive (red nuclei).

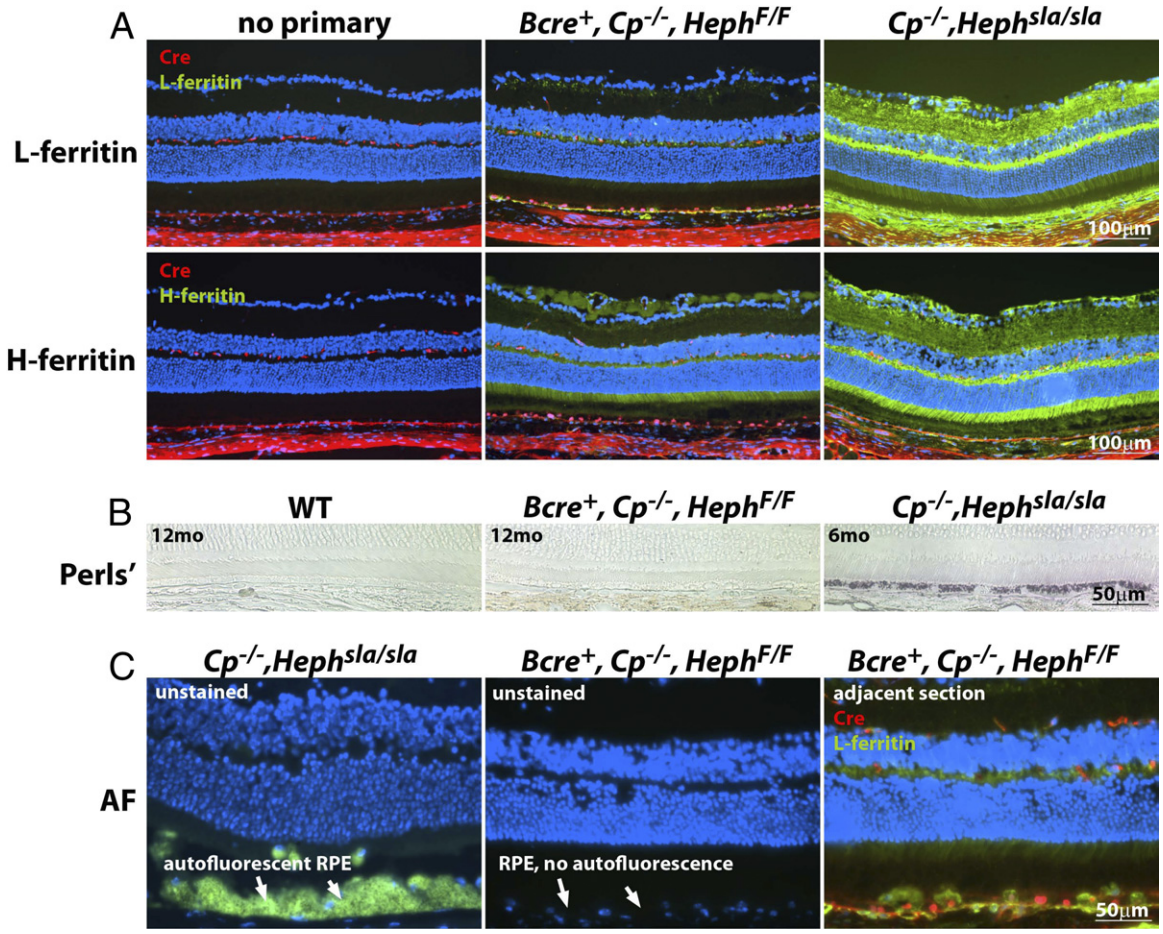

Figure 4. A: Iron levels, as determined by immunofluorescence for L- and H-ferritins, are not as great in *Bcre*$^{+}$, *Cp*$^{-/-}$, *Heph*$^{F/F}$ mice as they are in *Cp*$^{-/-}$, *Heph*$^{sla/sla}$ mice. **B:** VIP-enhanced Perls' stain for iron. *Cp*$^{-/-}$, *Heph*$^{sla/sla}$ mice accumulate iron in RPE cells that can be detected by VIP-enhanced Perls' stain at the age of 6 months, whereas iron cannot be detected with VIP-enhanced Perls' staining in *Bcre*$^{+}$, *Cp*$^{-/-}$, *Heph*$^{F/F}$ mice as late as the age of 12 months. **C:** RPE cells in *Cp*$^{-/-}$, *Heph*$^{sla/sla}$ mice are autofluorescent, whereas RPE cells in *Bcre*$^{+}$, *Cp*$^{-/-}$, *Heph*$^{F/F}$ mice are not autofluorescent, even though they are cre positive and have increased L-ferritin levels. The **arrows** point to the RPE cells. AF, autofluorescence.

These results suggested that photoreceptors that lack Cp and Heph can export iron via another mechanism. Photoreceptor cells produce the iron carriers transferrin and hemopexin.[19,20] We performed quantitative RT-PCR for these iron carriers on neural retinas of *Rcre*$^{+}$, *Cp*$^{-/-}$, *Heph*$^{F/F}$ and control mice and saw no changes in their levels (data not shown). In addition, the protein levels of the ferroxidase APP were unchanged, suggesting that there is yet another iron export mechanism that compensates for loss of Cp and Heph from photoreceptors.

To determine whether photoreceptors would accumulate iron if the RPE cells were iron laden, we generated *Rcre*$^{+}$, *Bcre*$^{+}$, *Cp*$^{-/-}$, *Heph*$^{F/F}$ mice that lacked Heph in both RPE and photoreceptor cells on a *Cp*$^{-/-}$ background. The RPE cells of these mice did not have increased iron levels by immunofluorescence for L-ferritin beyond the *Bcre*$^{+}$, *Cp*$^{-/-}$, *Heph*$^{F/F}$ controls; similarly, the photoreceptors did not have increased iron levels. However, the bipolar cells had increased L-ferritin levels (Figure 5, A and B). We confirmed that these were bipolar cells by immunostaining for L-ferritin and protein kinase Cα, a bipolar cell marker, or for glutamine synthetase, a Muller cell marker (Figure 5C). The difference in L-ferritin levels in *Rcre*$^{+}$, *Bcre*$^{+}$, *Cp*$^{-/-}$, *Heph*$^{F/F}$ retinas compared with *Bcre*$^{+}$, *Cp*$^{-/-}$, *Heph*$^{F/F}$ retinas indicates that Heph plays a role in photoreceptor cells, although it is a minor role.

Systemic Heph *Knockout Causes More Retinal Iron Accumulation than the* sla *Mutation*

Although the *Rcre*$^{+}$, *Bcre*$^{+}$, *Cp*$^{-/-}$, *Heph*$^{F/F}$ retinas had increased L-ferritin levels, they did not have nearly the same L-ferritin levels as the *Cp*$^{-/-}$, *Heph*$^{sla/sla}$ mice. This suggested that either the *sla* mutation causes more iron accumulation than *Heph* knockout or that Cp and Heph function may be more important in other cells of the retina than previously thought. To determine whether the *sla* mutation causes more retinal iron accumulation than the *Heph* knockout, we generated systemic *Heph* knockout mice by taking advantage of ectopic cre expression in the testes of occasional *Bcre*$^{+}$ mice.[14] *Heph* knockout mice (*Heph*$^{-/-}$) had evidence of *Heph* recombination by PCR in all somatic cells and loss of Heph protein in the retina (Figure 1D). At a young age, *Heph*$^{-/-}$ mice lacked body hair but had facial hair (Figure 6A), similar to previ-

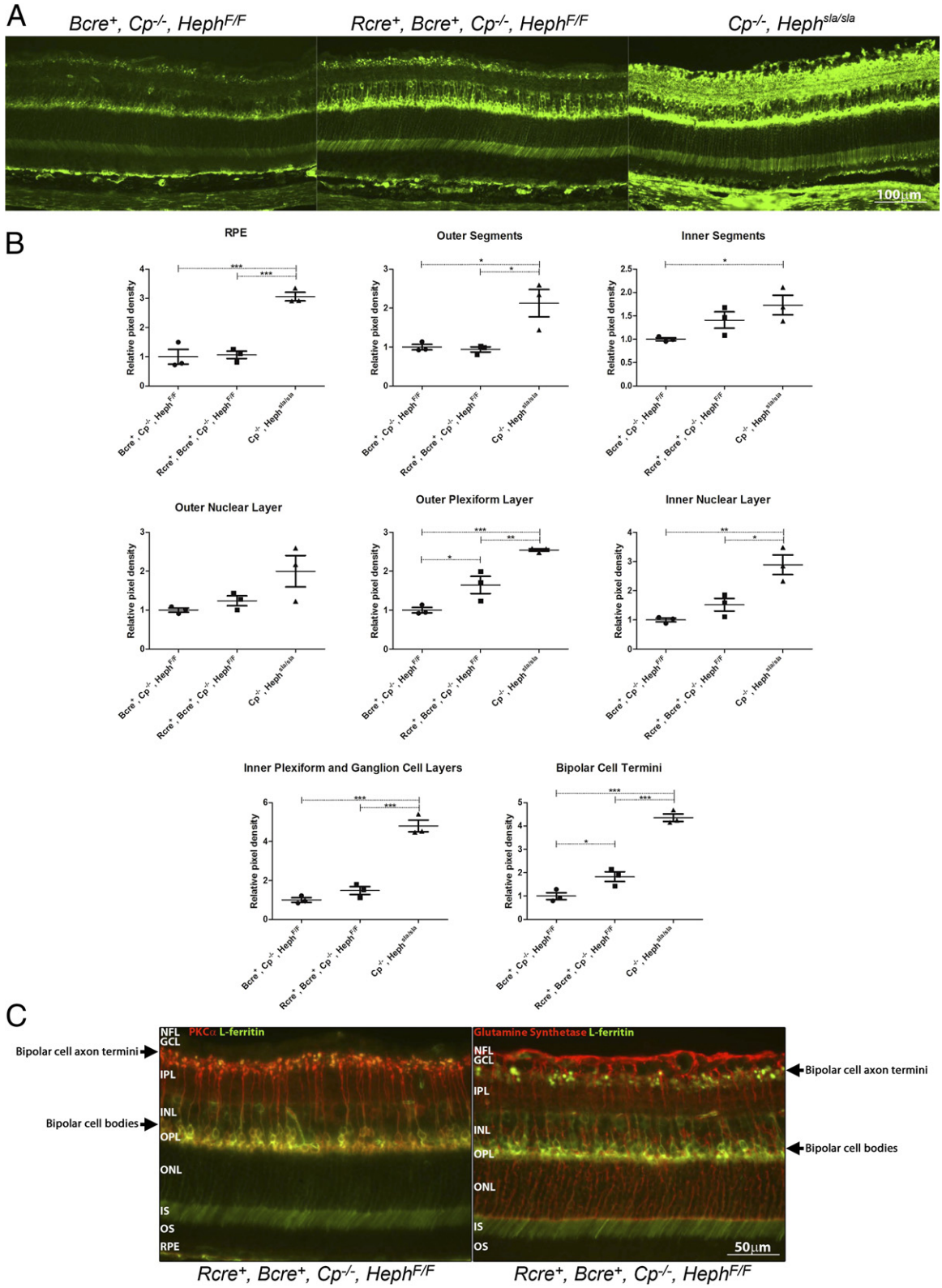

Figure 5. A: Representative images of L-ferritin immunofluorescence staining in 6-month-old *Bcre*$^{+}$, *Cp*$^{-/-}$, *Heph*$^{F/F}$ mice; Rcre^{+}, *Bcre*$^{+}$, *Cp*$^{-/-}$, *Heph*$^{F/F}$ mice; and *Cp*$^{-/-}$, *Heph*$^{sla/sla}$ mice. **B:** Pixel density quantification of L-ferritin immunostaining in the different retinal layers of three mice of each of the previously described genotypes. A one-way analysis of variance with a Tukey post test was used to compare the means between the groups. For each graph, *P* values comparing all three samples in each graph calculated using ANOVA are as follows: RPE, $P = 0.0003$; outer segments, $P = 0.119$; inner segments, $P = 0.0458$; outer nuclear layer, $P = 0.660$; outer plexiform layer, $P = 0.0006$; inner nuclear layer, $P = 0.0031$; inner plexiform and ganglion cell layers, $P < 0.0001$; bipolar cell termini, $P < 0.001$. Significant differences for pairwise comparisons calculated using the Tukey post-test are indicated on each graph. $^{*}P < 0.05$, $^{**}P < 0.01$, $^{***}P < 0.001$. **C:** L-Ferritin immunostaining colocalizes with protein kinase Cα, a bipolar cell marker, and not with glutamine synthetase, a Muller cell marker. GCL, ganglion cell layer; INL, inner nuclear layer; IPL, inner plexiform layer; IS, inner segments; NFL, nerve fiber layer; ONL, outer nuclear layer; OPL, outer plexiform layer; OS, outer segments.

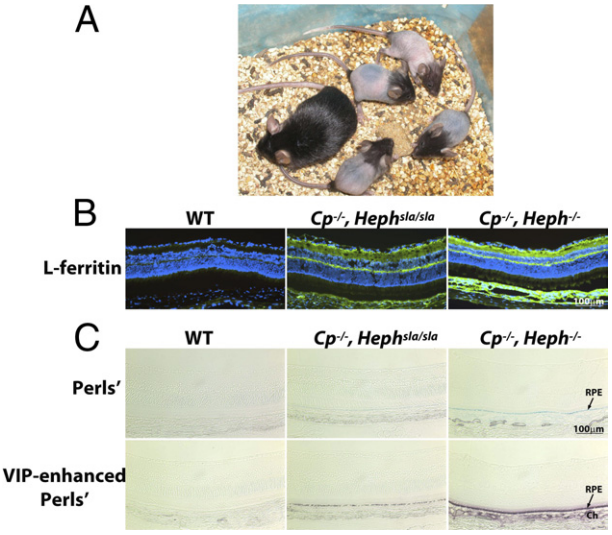

Figure 6. A: *Heph*$^{-/-}$ pups, aged 1 month, and their mother. The pups only have hair on the face and at the base of the tail, lacking body hair. **B:** Immunofluorescence for L-ferritin. *Cp*$^{-/-}$, *Heph*$^{-/-}$ mice have greater L-ferritin levels in the neural retina, RPE cells, and choroid than *Cp*$^{-/-}$, *Heph*$^{sla/sla}$ mice. **C:** Unenhanced Perls' stain for iron (blue) and VIP-enhanced Perls' stain for iron (purple). *Cp*$^{-/-}$, *Heph*$^{-/-}$ mice have greater iron levels in the RPE and choroid than do *Cp*$^{-/-}$, *Heph*$^{sla/sla}$ mice. Ch, choroid.

ously described masked mice with a mutation in the *Tmprss6* gene[21,22]; the hair would grow back after weaning.

The *Heph*$^{-/-}$ mice were bred to *Cp*$^{-/-}$ mice to generate *Cp*$^{-/-}$, *Heph*$^{-/-}$ mice. Like *Cp*$^{-/-}$, *Heph*$^{sla/sla}$ mice, the *Cp*$^{-/-}$, *Heph*$^{-/-}$ mice were anemic, with a hematocrit of 31 ± 5.7 (n = 4), and developed neurodegenerative symptoms, such as those seen in *Cp*$^{-/-}$, *Heph*$^{sla/sla}$ mice from the age of 3 months.[23] Compared with *Cp*$^{-/-}$, *Heph*$^{sla/sla}$ mice, *Cp*$^{-/-}$, *Heph*$^{-/-}$ mice had increased retinal iron levels by both immunofluorescence for ferritin and Perls' stain (Figure 6, B and C). The Perls' stain was prominent in the RPE cells and the choroid. This confirmed that *Heph* knockout causes more retinal iron accumulation than *Heph* mutation, that Cp and Heph are not necessary for retinal iron import but are necessary for retinal iron export, and that Cp and Heph likely play an important role in other retinal cells.

Muller Cells Express Ferroxidases Cp, Heph, APP, and Zp

Muller cells are well positioned to regulate retinal iron levels because they span the thickness of the entire retina and are close to the retinal blood vessels. To determine which ferroxidases are expressed by Muller cells, we cultured primary Muller cells. Primary Muller cell identity was verified by immunostaining and quantitative RT-PCR, as previously described.[17] In primary Muller cells, Cp, Heph, APP, and Zp ferroxidase mRNA was detected by quantitative RT-PCR, whereas in isolated RPE cells, Cp, Heph, and APP were detected but Zp was not. Ferroportin mRNA was detected in both primary Muller cells and isolated RPE cells.

Discussion

Heph Plays a Cell-Autonomous Role in RPE Cells

Our current studies demonstrate that Heph plays a cell-autonomous role in RPE cells, because loss of Heph from RPE cells alone on a *Cp*$^{-/-}$ background causes RPE cell iron accumulation and pathological features (Figures 2 and 3). Ferritin accumulated only in RPE cells expressing cre, which, based on Western blot analysis of retinas from systemic *Heph*$^{-/-}$ mice, causes loss of Heph protein. Loss of Heph from other cells in the retina is not necessary to cause these RPE changes. The increased L-ferritin levels in RPE cells of *Bcre*$^{+}$, *Cp*$^{-/-}$, *Heph*$^{F/F}$ mice are moderate and are much lower than the levels in systemic *Cp*$^{-/-}$, *Heph*$^{sla/sla}$ and *Cp*$^{-/-}$, *Heph*$^{-/-}$ knockout mice (Figure 4). These results indicate that RPE cells are sensitive to cellular iron levels, because moderate increases in iron levels are sufficient to cause RPE cell pathological characteristics. Both Cp and Heph are important for RPE cell iron export and have somewhat redundant iron export roles; when RPE cells lack Heph or Cp alone, there is no change in RPE cell L-ferritin levels and no RPE pathological features. In addition to Cp and Heph, isolated RPE cells expressed APP but not Zp mRNA, suggesting that three ferroxidases (Cp, Heph, and APP) may be used by RPE cells. The role of APP in RPE iron export is unclear.

RPE Cells Accept Iron from Other Iron-Overloaded Cells

Although *Bcre*$^{+}$, *Cp*$^{-/-}$, *Heph*$^{F/F}$ mice have increased RPE iron levels, these levels are much lower than in *Cp*$^{-/-}$, *Heph*$^{sla/sla}$ RPE, suggesting that loss of Heph function in the cells of the neural retina is necessary for the large RPE cell iron accumulation in the systemic knockout mice. Similar high levels of RPE iron accumulation are seen in mice with systemic knockout of *BMP6* and *hepcidin*, which are genes that are important for regulating cellular iron levels, and in humans with aceruloplasminemia.[6,17,18] Similar iron-handling mechanisms may be responsible for the greatly increased iron levels in the RPE cells of these different models. In the *Cp*$^{-/-}$, *Heph*$^{sla/sla}$ mice, loss of Heph and Cp from the neural retina may prevent iron export from the neural retina to the retinal vasculature or vitreous, increasing iron levels in the neural retina. The iron-overloaded neural retina may preferentially transfer the excess iron to the RPE cells as a protective mechanism when it cannot export enough iron to the retinal vasculature. Such transfer would be beneficial to the neural retina in several ways, including the preservation of the optical properties of the retina. In most cell types, excess iron accumulates as ferritin; in cases of extreme iron overload, it accumulates as hemosiderin.[24] Hemosiderin accumulation in the cells of the neural retina, however, can interfere with the optical properties of the cells of the neural retina,[25,26] whereas similar accumulation in RPE cells should not be as harmful.

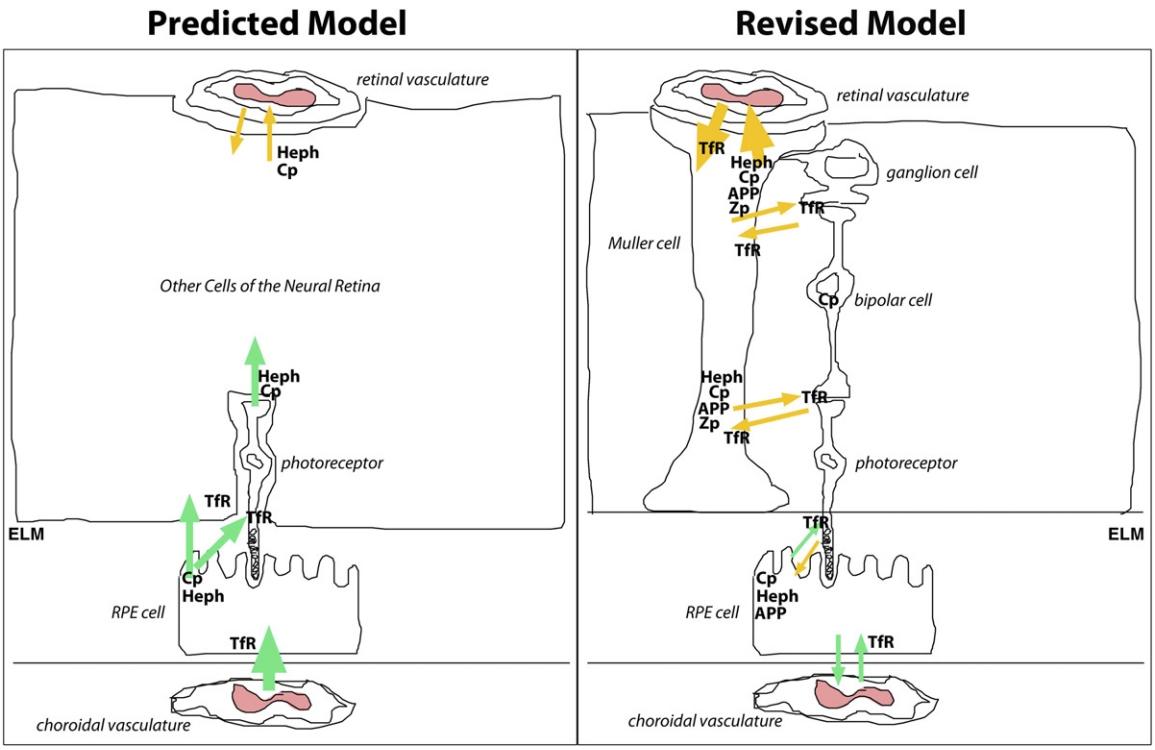

Figure 7. Predicted model of retinal iron transport before our current studies and revised model of retinal iron transport after our current studies. Before our current studies, we hypothesized that a large portion of iron that enters the neural retina comes from the choroidal circulation via RPE cells (**green arrows**). We also hypothesized that some iron in the neural retina is from the retinal vasculature (**gold arrows**). In addition, we did not know which retinal cells express the ferroxidases Cp, Heph, APP, and Zp. From our current studies, we determined that the RPE cells express Cp, Heph, and APP, but not Zp, and that Muller cells express transferrin receptor (TfR), ferroportin, Cp, Heph, APP, and Zp. We found that Cp and Heph are important for iron export from the neural retina but not for iron import into the neural retina. Our current studies support a model in which the retina is divided into two compartments, the Muller and RPE cell compartments, with Muller and RPE cells regulating iron levels in their respective compartments. The external limiting membrane (ELM) separates the two compartments. Our studies suggest that the choroidal vasculature mainly supplies iron to the RPE compartment (**green arrows**), whereas the retinal vasculature supplies iron to the Muller compartment via the Muller cells (**gold arrows**).

Heph Plays a Minor Role in Photoreceptor Cells and Muller Cells May Be Central to Retinal Iron Transport

Because ferritin levels are increased in the photoreceptors of $Cp^{-/-}$, $Heph^{sla/sla}$ mice, and RPE cells phagocytose large portions of photoreceptors daily, we hypothesized that phagocytosis of iron-laden photoreceptor outer segments by RPE cells may be a mechanism for iron loading of RPE cells in $Cp^{-/-}$, $Heph^{sla/sla}$ mice and that Heph and Cp are important for photoreceptor iron export. We hypothesized that knocking out *Heph* and *Cp* from photoreceptor cells would result in photoreceptor iron increases, similar to what is seen in RPE cells. However, we found that in $Rcre^{+}$, $Cp^{-/-}$, $Heph^{F/F}$ mice, photoreceptor iron levels were unchanged, suggesting that *Heph* and *Cp* do not play a major role for photoreceptor iron export. Knocking *Heph* out of both RPE and photoreceptor cells on a $Cp^{-/-}$ background, however, results in changes in retinal L-ferritin levels (Figure 5), indicating that Heph plays a role in photoreceptor iron export, although the role is minor. Thus, the high iron accumulation in the retinas and RPE of systemic $Cp^{-/-}$, $Heph^{sla/sla}$ and $Cp^{-/-}$, $Heph^{-/-}$ mice is a result of lack of Heph function in retinal cells other than photoreceptors and RPE. The retinal iron accumulation in $Cp^{-/-}$, $Heph^{sla/sla}$ mice is not a consequence of elevated circulating iron levels; indeed, transferrin saturation and blood iron levels are low in $Cp^{-/-}$, $Heph^{sla/sla}$ mice (M. Hadziahmetovic, J.L. Dunaief, unpublished data).

Muller cells may be central to regulation of retinal iron levels because Muller cells express four ferroxidases (Cp, Heph, APP, and Zp). They express the iron exporter ferroportin, they produce the iron-regulatory hormone hepcidin,[27] and they are ideally positioned for regulating retinal iron transfer. Muller cells span the entire thickness of the retina and wrap around the photoreceptor, bipolar, and ganglion cells of the neural retina, separating them from the retinal blood vessels.[28,29] Thus, iron that is transported from the retinal vasculature to the photoreceptor, bipolar, or ganglion cells, or iron that is transported from these cells to the retinal vasculature, most likely traverses the Muller cells. Thus, Muller cells may regulate the iron flux between the neural retina and the retinal vasculature (Figure 7). In $Cp^{-/-}$, $Heph^{sla/sla}$ mice, decreased iron export by Muller cells to the retinal vasculature may increase labile iron levels in Muller cells, causing them, in turn, to down-regulate transferrin receptor and absorb less iron from the photoreceptor, bipolar, and ganglion cells. This would leave more holotransferrin in the space surrounding the photoreceptor, bipolar, and ganglion cells, causing them to eventually be iron overloaded.

Such a model of retinal iron handling, in which Muller cells play a central role, is in agreement with a recently proposed model of the retina, in which the retina is divided into two compartments based on the support cells of the retina, RPE and Muller cells.[29] The dividing line between the two compartments is at the external limiting membrane (Figure 7). The photoreceptor inner and outer segments are located in the RPE cell compartment, whereas the rest of the photoreceptor, bipolar, and ganglion cells are embedded in the Muller compartment. Each type of support cell regulates the levels of iron and other nutrients in its own compartment and regulates the entrance and exit of these nutrients from its own blood supply. The choroidal vasculature supplies the RPE compartment, and the retinal vasculature supplies the Muller compartment. The normal exchange of iron between the two compartments may be minimal; however, in pathological situations, it may be increased. In support of the compartment model, our studies demonstrate that loss of ferroxidase function in RPE cells mostly affects the RPE cells and not the rest of the neural retina (Figures 2 and 3). In addition, a recent study[30] demonstrated that when ^{55}Fe-transferrin is injected intravitreally, the iron is distributed to all layers of the neural retina but not to the RPE cells or the choroid.

Although our studies primarily focused on RPE, photoreceptor, bipolar, and Muller cells, the retina also has several other retinal cell types (Figure 1A), including retinal astrocytes, horizontal cells, and amacrine cells. These cells likely also participate in iron transport, although their role in retinal iron transport is unclear.

Heph and Cp Are Necessary for Iron Export from the Retina but Not for Iron Import into the Retina

Before our current studies, it was unclear from the $Cp^{-/-}$, $Heph^{sla/sla}$ mice if Heph is necessary for iron import into the retina because there is residual ferroxidase activity in $Heph^{sla/sla}$ cells.[31] Interestingly, the $Cp^{-/-}$, $Heph^{-/-}$ mice had greater retinal iron accumulation than the $Cp^{-/-}$, $Heph^{sla/sla}$ mice, demonstrating that Cp and Heph are not necessary for iron export from the retinal vascular endothelial cells into the retina, but that Cp and Heph are necessary for iron export from the neural retina to the retinal vasculature or vitreous humor. These data suggest that Cp and Heph have a greater role in iron export from the neural retina than from the retinal vasculature. In addition, they suggest a role for the ferroxidases APP and Zp for iron export from the retinal vasculature to the neural retina. Although retinal vascular endothelial cells can transport iron by transferrin and ferritin transcytosis,[32,33] these are likely minor transport pathways. Ferroportin-mediated iron export from the retinal vascular endothelial cells into the neural retina is likely the major iron transport mechanism; when cultured retinal vascular endothelial cells are treated with hepcidin, iron export greatly diminishes from these cells.[18] This indicates that transferrin and ferritin transcytosis cannot compensate for ferroportin-mediated iron export from the retinal vasculature. Because Cp and Heph seem to play a minor role for iron export from the retinal vascular endothelial cells, the ferroxidases APP and Zp are likely the ferroxidases used for ferroportin-mediated iron export from the retinal vasculature to the neural retina. Specifically, APP may play an important role because retinal vascular endothelial cells express APP.[18,34]

Cells of the Neural Retina Do Not Require Iron from the Choroidal Vasculature

Before our current studies, much evidence indicated a possible transfer of iron from the choroid to the RPE cells and then to the neural retina (Figure 7). The choroid and RPE cells have the greatest iron levels in the normal retina, generating a gradient along which iron could be transferred to the rest of the retina.[35] In addition, RPE and photoreceptor cells express transferrin receptor, and both make the iron carrier transferrin.[36–39] This expression has been interpreted as evidence that RPE cells take up iron from the choroid and export it into the space between the RPE and photoreceptors, where iron then binds to transferrin and is then taken up by photoreceptor cells. Photoreceptors may then transfer the iron to other retinal cells (Figure 7). We found that iron from the choroid is likely only a minor source of iron for the neural retina because neural retinas from $Bcre^{+}$, $Cp^{-/-}$, $Heph^{F/F}$ mice, in which RPE cells have impaired iron export abilities, have decreased transferrin receptor levels and no changes in L-ferritin levels (Figure 2). These findings indicate that the neural retina is not iron deficient (which would have been expected if the neural retina depended on iron transport from the choroid) and may have increased levels of labile iron. The RPE-autonomous function of Heph is demonstrated herein, but clearly other retinal cells depend on Heph for iron transport. Overall, these studies support a new model of retinal iron transport. Future studies will define these additional Heph-dependent retinal cell types and iron transport routes.

References

1. Syed BA, Beaumont NJ, Patel A, Naylor CE, Bayele HK, Joannou CL, Rowe PS, Evans RW, Srai SK: Analysis of the human hephaestin gene and protein: comparative modelling of the N-terminus ecto-domain based upon ceruloplasmin. Protein Eng 2002, 15:205–214
2. Vulpe CD, Kuo YM, Murphy TL, Cowley L, Askwith C, Libina N, Gitschier J, Anderson GJ: Hephaestin, a ceruloplasmin homologue implicated in intestinal iron transport, is defective in the sla mouse. Nat Genet 1999, 21:195–199
3. De Domenico I, Ward DM, di Patti MC, Jeong SY, David S, Musci G, Kaplan J: Ferroxidase activity is required for the stability of cell surface ferroportin in cells expressing GPI-ceruloplasmin. EMBO J 2007, 26:2823–2831
4. Hahn P, Qian Y, Dentchev T, Chen L, Beard J, Harris ZL, Dunaief JL: Disruption of ceruloplasmin and hephaestin in mice causes retinal iron overload and retinal degeneration with features of age-related macular degeneration. Proc Natl Acad Sci U S A 2004, 101:13850–13855
5. Moiseyev G, Takahashi Y, Chen Y, Gentleman S, Redmond TM, Crouch RK, Ma JX: RPE65 is an iron(II)-dependent isomerohydrolase in the retinoid visual cycle. J Biol Chem 2006, 281:2835–2840

6. Wolkow N, Song Y, Wu T, Qian J, Guerquin-Kern J, Dunaief JL: Aceruloplasminemia: retinal histopathologic manifestations and iron-mediated melanosome degradation. Arch Ophthalmol 2011, 129: 1466–1474
7. Hahn P, Milam AH, Dunaief JL: Maculas affected by age-related macular degeneration contain increased chelatable iron in the retinal pigment epithelium and Bruch's membrane. Arch Ophthalmol 2003, 121:1099–1105
8. Young RW: The renewal of photoreceptor cell outer segments. J Cell Biol 1967, 33:61–72
9. McBee JK, Palczewski K, Baehr W, Pepperberg DR: Confronting complexity: the interlink of phototransduction and retinoid metabolism in the vertebrate retina. Prog Retin Eye Res 2001, 20:469–529
10. Gal A, Li Y, Thompson DA, Weir J, Orth U, Jacobson SG, Apfelstedt-Sylla E, Vollrath D: Mutations in MERTK, the human orthologue of the RCS rat retinal dystrophy gene, cause retinitis pigmentosa. Nat Genet 2000, 26:270–271
11. Gu SM, Thompson DA, Srikumari CR, Lorenz B, Finckh U, Nicoletti A, Murthy KR, Rathmann M, Kumaramanickavel G, Denton MJ, Gal A: Mutations in RPE65 cause autosomal recessive childhood-onset severe retinal dystrophy. Nat Genet 1997, 17:194–197
12. Chen L, Dentchev T, Wong R, Hahn P, Wen R, Bennett J, Dunaief JL: Increased expression of ceruloplasmin in the retina following photic injury. Mol Vis 2003, 9:151–158
13. Patel BN, Dunn RJ, Jeong SY, Zhu Q, Julien JP, David S: Ceruloplasmin regulates iron levels in the CNS and prevents free radical injury. J Neurosci 2002, 22:6578–6586
14. Iacovelli J, Zhao C, Wolkow N, Veldman P, Gollomp K, Ojha P, Lukinova N, King A, Feiner L, Esumi N, Zack DJ, Pierce EA, Vollrath D, Dunaief JL: Generation of Cre transgenic mice with postnatal RPE-specific ocular expression. Invest Ophthalmol Vis Sci 2011, 52: 1378–1383
15. Le YZ, Zheng L, Zheng W, Ash JD, Agbaga MP, Zhu M, Anderson RE: Mouse opsin promoter-directed Cre recombinase expression in transgenic mice. Mol Vis 2006, 12:389–398
16. Harris ZL, Durley AP, Man TK, Gitlin JD: Targeted gene disruption reveals an essential role for ceruloplasmin in cellular iron efflux. Proc Natl Acad Sci U S A 1999, 96:10812–10817
17. Hadziahmetovic M, Song Y, Wolkow N, Iacovelli J, Kautz L, Roth MP, Dunaief JL: Bmp6 regulates retinal iron homeostasis and has altered expression in age-related macular degeneration. Am J Pathol 2011, 179:335–348
18. Hadziahmetovic M, Song Y, Ponnuru P, Iacovelli J, Hunter A, Haddad N, Beard J, Connor JR, Vaulont S, Dunaief JL: Age-dependent retinal iron accumulation and degeneration in hepcidin knockout mice. Invest Ophthalmol Vis Sci 2011, 52:109–118
19. Davis AA, Hunt RC: Transferrin is made and bound by photoreceptor cells. J Cell Physiol 1993, 156:280–285
20. Chen W, Lu H, Dutt K, Smith A, Hunt DM, Hunt RC: Expression of the protective proteins hemopexin and haptoglobin by cells of the neural retina. Exp Eye Res 1998, 67:83–93
21. Du X, She E, Gelbart T, Truksa J, Lee P, Xia Y, Khovananth K, Mudd S, Mann N, Moresco EM, Beutler E, Beutler B: The serine protease TMPRSS6 is required to sense iron deficiency. Science 2008, 320: 1088–1092
22. Folgueras AR, de Lara FM, Pendas AM, Garabaya C, Rodriguez F, Astudillo A, Bernal T, Cabanillas R, Lopez-Otin C, Velasco G: Membrane-bound serine protease matriptase-2 (Tmprss6) is an essential regulator of iron homeostasis. Blood 2008, 112:2539–2545
23. Hadziahmetovic M, Dentchev T, Song Y, Haddad N, He X, Hahn P, Pratico D, Wen R, Harris ZL, Lambris JD, Beard J, Dunaief JL: Ceruloplasmin/hephaestin knockout mice model morphologic and molecular features of AMD. Invest Ophthalmol Vis Sci 2008, 49:2728–2736
24. Harrison PM, Arosio P: The ferritins: molecular properties, iron storage function and cellular regulation. Biochim Biophys Acta 1996, 1275:161–203
25. Solovei I, Kreysing M, Lanctot C, Kosem S, Peichl L, Cremer T, Guck J, Joffe B: Nuclear architecture of rod photoreceptor cells adapts to vision in mammalian evolution. Cell 2009, 137:356–368
26. Franze K, Grosche J, Skatchkov SN, Schinkinger S, Foja C, Schild D, Uckermann O, Travis K, Reichenbach A, Guck J: Muller cells are living optical fibers in the vertebrate retina. Proc Natl Acad Sci U S A 2007, 104:8287–8292
27. Gnana-Prakasam JP, Martin PM, Mysona BA, Roon P, Smith SB, Ganapathy V: Hepcidin expression in mouse retina and its regulation via lipopolysaccharide/Toll-like receptor-4 pathway independent of Hfe. Biochem J 2008, 411:79–88
28. Hogan MJ, Alvarado JA, Weddell JE: Histology of the Human Eye: An Atlas and Textbook. Philadelphia, Saunders, 1971
29. Sisak S, Banin E, Blumenthal EZ: A two-compartment model of the human retina. Med Hypotheses 2004, 62:808–816
30. Moos T, Bernth N, Courtois Y, Morgan EH: Developmental iron uptake and axonal transport in the retina of the rat. Mol Cell Neurosci 2011, 46:607–613
31. Chen H, Attieh ZK, Su T, Syed BA, Gao H, Alaeddine RM, Fox TC, Usta J, Naylor CE, Evans RW, McKie AT, Anderson GJ, Vulpe CD: Hephaestin is a ferroxidase that maintains partial activity in sex-linked anemia mice. Blood 2004, 103:3933–3939
32. Burdo JR, Antonetti DA, Wolpert EB, Connor JR: Mechanisms and regulation of transferrin and iron transport in a model blood-brain barrier system. Neuroscience 2003, 121:883–890
33. Fisher J, Devraj K, Ingram J, Slagle-Webb B, Madhankumar AB, Liu X, Klinger M, Simpson IA, Connor JR: Ferritin: a novel mechanism for delivery of iron to the brain and other organs. Am J Physiol Cell Physiol 2007, 293:C641–C649
34. Chen ST, Patel AJ, Garey LJ, Jen LS: Expression of beta-amyloid precursor protein immunoreactivity in the retina of the rat during normal development and after neonatal optic tract lesion. Neuroreport 1997, 8:713–717
35. Yefimova MG, Jeanny JC, Keller N, Sergeant C, Guillonneau X, Beaumont C, Courtois Y: Impaired retinal iron homeostasis associated with defective phagocytosis in Royal College of Surgeons rats. Invest Ophthalmol Vis Sci 2002, 43:537–545
36. Yefimova MG, Jeanny JC, Guillonneau X, Keller N, Nguyen-Legros J, Sergeant C, Guillou F, Courtois Y: Iron, ferritin, transferrin, and transferrin receptor in the adult rat retina. Invest Ophthalmol Vis Sci 2000, 41:2343–2351
37. Sugasawa K, Deguchi J, Okami T, Yamamoto A, Omori K, Uyama M, Tashiro Y: Immunocytochemical analyses of distributions of Na, K-ATPase and GLUT1, insulin and transferrin receptors in the developing retinal pigment epithelial cells. Cell Struct Funct 1994, 19:21–28
38. Hunt RC, Dewey A, Davis AA: Transferrin receptors on the surfaces of retinal pigment epithelial cells are associated with the cytoskeleton. J Cell Sci 1989, 92(Pt 4):655–666
39. Hunt RC, Davis AA: Release of iron by human retinal pigment epithelial cells. J Cell Physiol 1992, 152:102–110